

Amino Acid Residues Outside of the Pore Region Contribute to N-type Calcium Channel Permeation*

Received for publication, November 8, 2000, and in revised form, December 15, 2000
Published, JBC Papers in Press, December 18, 2000, DOI 10.1074/jbc.C000791200

Zhong-Ping Feng^{‡§¶}, Jawed Hamid[‡], Clinton Doering^{‡§}, Scott E. Jarvis^{‡¶}, Gregory M. Bosey^{**},
Emmanuel Bourinet^{‡‡}, Terry P. Snutch^{**§§}, and Gerald W. Zamponi^{‡¶¶}

From the [‡]Departments of Physiology and Biophysics and Pharmacology and Therapeutics, Neuroscience Research Group, University of Calgary, Calgary T2N 4N1, Canada, [§]NeuroMed Technologies Inc., Vancouver V6T 1Z4, Canada, ^{**}Biotechnology Laboratory, University of British Columbia, Vancouver V6T 1Z3, Canada, and ^{‡‡}Institute of Human Genetics, CNRS, Montpellier, 34094 France

It is widely believed that the selectivity of voltage-dependent calcium channels is mainly controlled by amino acid residues contained within four p-loop motifs forming the pore of the channel. An examination of the amino acid sequences of high voltage-activated calcium channels reveals that their domain III S5–H5 regions contain a highly conserved motif with homology to known EF hand calcium binding proteins, hinting that this region may contribute to channel permeation. To test this hypothesis, we used site-directed mutagenesis to replace three conserved negatively charged residues in the N-type calcium channel α_{1B} subunit (Glu-1321, Asp-1323, and Glu-1332) with positively charged amino acids (lysine and arginine) and studied their effect on ion selectivity using whole cell and single channel patch clamp recordings. Whereas the wild type channels conducted barium much more effectively than calcium, the mutant displayed nearly equal permeabilities for these two ions. Individual replacement of residue 1332 or a double substitution of residues 1321 and 1323 with lysine and arginine, respectively, were equally effective. Disruption of the putative EF hand motif through replacement of the central glycine residue (1326) with proline resulted in a similar effect, indicating that the responses observed with the triple mutant were not due to changes in the net charge of the channel. Overall, our data indicate that residues outside of the narrow region of the pore have the propensity to contribute to calcium channel permeation. They also raise the possibility that interactions of calcium ions with a putative calcium binding domain at the extracellular side of the channel may underlie the differential permeabilities of the channel for barium and calcium ions.

The influx of calcium ions through voltage-gated calcium channels mediates a wide range of cellular responses, including the activation of calcium-dependent enzymes, gene transcription, muscle contraction, and the release of neurotransmitter. Under physiological conditions, calcium channels are highly selective for calcium; however, they are also capable of permeating other types of non-physiological cations such as barium and strontium (1). Most types of high voltage-activated calcium channels (*i.e.* the L-, P/Q-, and N-types) conduct barium about 1.5- to 2-fold more effectively than calcium, whereas T-type and R-type calcium channels conduct calcium as well as, or slightly better than, barium (1–4). The primary loci of ion selectivity in voltage-dependent calcium channels appear to reside within the p-loop motifs of each of the four transmembrane domains of the calcium channel α_1 subunit (5–7). Each of the p-loops contains a conspicuous glutamic acid residue that is conserved among all types of high voltage-activated calcium channels. Mutation of either of these residues severely impairs calcium permeation (5, 6, 8, 9), and insertion of these glutamates at corresponding positions into a voltage-dependent sodium channel confers calcium selectivity (10). However, the observations that R-type and other types of non-T-type calcium channels show opposing relative selectivities for barium and calcium ions cannot be easily explained by an exclusive involvement of the four glutamate residues, because they are entirely conserved in these channel subtypes. It is conceivable that the relative three-dimensional arrangement of the amino acid side chains within the four p-loops is not the same in all calcium channel subtypes and thus accounts for the different permeation profiles (11). Alternatively, it is possible that voltage-dependent calcium channels contain an additional, yet to be identified locus that controls ion selectivity. For example, we have previously proposed that voltage-dependent calcium channels contain an extracellular calcium binding site that is linked to the activation gating machinery of the channel (12) and that may affect channel permeation.

Here, we report that the domain III S5–H5 regions of all types of high voltage-activated calcium channels contain a putative EF hand motif, a central glycine residue flanked by three negatively charged residues, which is homologous to calcium binding domains of known calcium binding proteins. We show that substitution of these highly conserved negative charges with arginine/lysine or replacement of the central glycine by proline in the N-type calcium channel α_1 subunit dramatically reduces the difference in barium and calcium conductance seen with the wild type channel. Thus, residues far outside the narrow region of the N-type calcium channel pore contribute in a significant manner to the permeation properties of the channel.

* This work was supported by an operating grant (to G. W. Z.) from the Canadian Institutes of Health Research (CIHR), the Heart and Stroke Foundation of Alberta and the Northwest Territories, a collaborative NATO travel grant (to G. W. Z. and E. B.), and through a scholarship award (to G. W. Z.) from the EJLB Foundation. The costs of publication of this article were defrayed in part by the payment of page charges. This article must therefore be hereby marked "advertisement" in accordance with 18 U.S.C. Section 1734 solely to indicate this fact.

¶ Holds a postdoctoral fellowship from the Natural Science and Engineering Research Council of Canada.

¶ Recipient of an Alberta Heritage Foundation for Medical Research (AHFMR) studentship award.

§§ Supported through CIHR operating funds and a Senior Scientist award from the CIHR.

¶¶ Holds faculty scholarships from AHFMR and the CIHR and is the Novartis Investigator in Schizophrenia Research. To whom correspondence should be addressed: Dept. of Physiology and Biophysics, University of Calgary, 3330 Hospital Dr. NW, Calgary, Alberta T2N 4N1, Canada. Tel.: 403-220-8687; Fax: 403-210-8106; E-mail: Zamponi@ucalgary.ca.

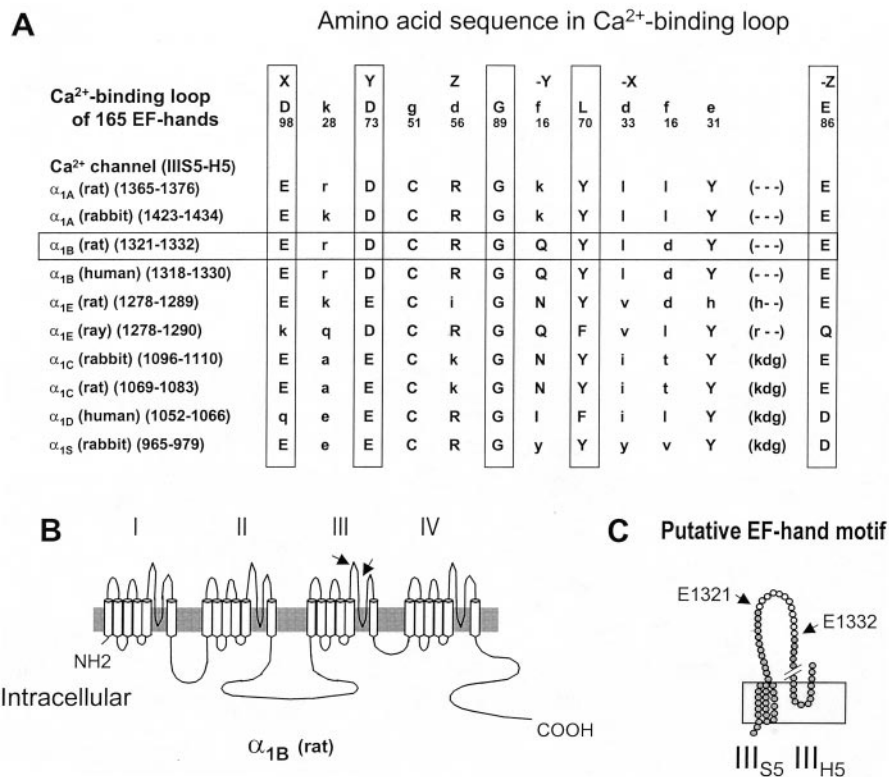


FIG. 1. A, amino acid alignment of the domain III S5–H5 region of various calcium channel α_1 subunit isoforms (13) in comparison with a signature EF hand calcium binding motif common to 165 different calcium binding proteins (14). The numerical values indicate the incidence of this particular residue among the 165 motifs. Note that similar to EF hand motifs, most voltage-activated calcium channels contain a central glycine flanked by three negatively charged residues in their III S5–H5 region. B and C, proposed transmembrane topology of the calcium channel α_1 subunit (15) indicating the location of the putative EF hand motif.

MATERIALS AND METHODS

Tissue Culture and Transient Transfection—Human embryonic kidney tsa-201 cells were maintained in a 37 °C CO₂ incubator in standard DMEM¹ supplemented with 10% fetal bovine serum, 200 units/ml penicillin, and 0.2 mg/ml streptomycin. At 85% confluency, the cells were split with trypsin EDTA and plated on glass coverslips at 10% confluency. The cells were allowed to recover for 12 h at 37 °C. The medium was then replaced, and the cells were transiently transfected with cDNAs encoding for calcium channel α_{1B} , β_{1B} , and $\alpha_2\text{-}\delta$ subunits and enhanced green fluorescent protein at a 1:1:1:0.3 molar ratio, using a standard calcium phosphate protocol. After 12 h, the medium was replaced with fresh DMEM. The cells were allowed to recover for additional 12 h and subsequently stored at 28 °C in 5% CO₂ for 1–2 days prior to recording.

Site-directed Mutagenesis—A 4.5-kilobase *SpI*-*Afl*II fragment was excised from the full-length α_{1B} construct contained in a CMV expression vector and ligated into pSL1180. Site-directed mutagenesis was carried out on this construct via the Quik Change mutagenesis kit (Stratagene) according to the instructions provided by the manufacturer. Successful mutagenesis and absence of undesired sequence errors was confirmed via DNA sequencing. Subsequently, the mutant *SpI*-*Afl*II fragment was reintroduced into the full-length clone in CMV. Incorporation of the mutated fragment in the full-length clone was verified by restriction endonuclease digestion and DNA sequencing.

Electrophysiology—Single channel recordings (cell attached) and whole cell patch clamp (ruptured) recordings were performed using an Axopatch 200B amplifier (Axon Instruments, Foster City, CA) linked to a personal computer equipped with pClamp, Version 7.0. Patch pipettes (Sutter borosilicate glass, BF 150–86-15) were pulled using a Sutter P-87 microelectrode puller and subsequently fire polished using a Narashige microforge.

For single channel recordings, pipettes were coated with sylgard and filled with solution containing 100 mM BaCl₂ (or CaCl₂) and 10 mM HEPES (pH 7.2 with CsOH). Pipette resistance was typically in the range of 10–20 megohms. Cells were transferred to a 3-cm culture dish

containing solution comprised of 140 mM sodium gluconate, 1 mM MgCl₂, 10 mM HEPES, 10 mM EGTA, and 10 mM glucose (pH 7.3 adjusted with KOH). Currents were elicited by stepping from a holding potential of –100 mV (physiological) to various test depolarizations. Data were sampled at 5 kHz and filtered at 1 kHz.

For whole cell current recording, pipettes (in the range of 2–4 megohms) were filled with internal solution containing 108 mM cesium methanesulfonate, 4 mM MgCl₂, 9 mM EGTA, 9 mM HEPES (pH 7.2 adjusted with tetraethylammonium hydroxide). The cells were transferred to a 3-cm culture dish containing recording solution comprised of 20 mM BaCl₂ (or CaCl₂), 1 mM MgCl₂, 10 mM HEPES, 40 mM tetraethylammonium chloride, 10 mM glucose, 87.5 mM CsCl (pH 7.2 adjusted with tetraethylammonium hydroxide). Currents were elicited by stepping from a holding potential of –100 mV to various test potentials using Clampex software. Cadmium was dissolved in the external recording solution and perfused onto the cells at various concentrations using a gravity-driven perfusion system. Data were filtered at 1 kHz using a 4-pole Bessel filter and digitized at a sampling frequency of 2 kHz. Data were analyzed using Clampfit (Axon Instruments). Cadmium dose-response curves were fitted with the Hill equation. All curve fittings were carried out using Sigmaplot 4.0 (Jandel Scientific).

Statistics—Statistical analysis was carried out using SigmaStat 2.0 (Jandel Scientific). Differences between mean values from each experimental group were tested using a Student's *t* test for two groups and one-way analysis of variance (ANOVA) for multiple comparisons. Differences were considered significant if *p* < 0.05.

RESULTS AND DISCUSSION

Fig. 1 shows a sequence alignment of the domain III S5–H5 region of various high voltage-activated calcium channels (13) with a common motif found in many types of calcium binding proteins, a central glycine residue flanked by three negative charges (14). As is evident from the alignment, the central glycine residue is conserved in all types of high voltage-activated calcium channels. Furthermore, with the exception of the marine ray α_{1E} and the human α_{1D} channels, the three critical negatively charged residues are also conserved. This raises the possibility

¹ The abbreviations used are: DMEM, Dulbecco's modified Eagle's medium; CMV, cytomegalovirus.

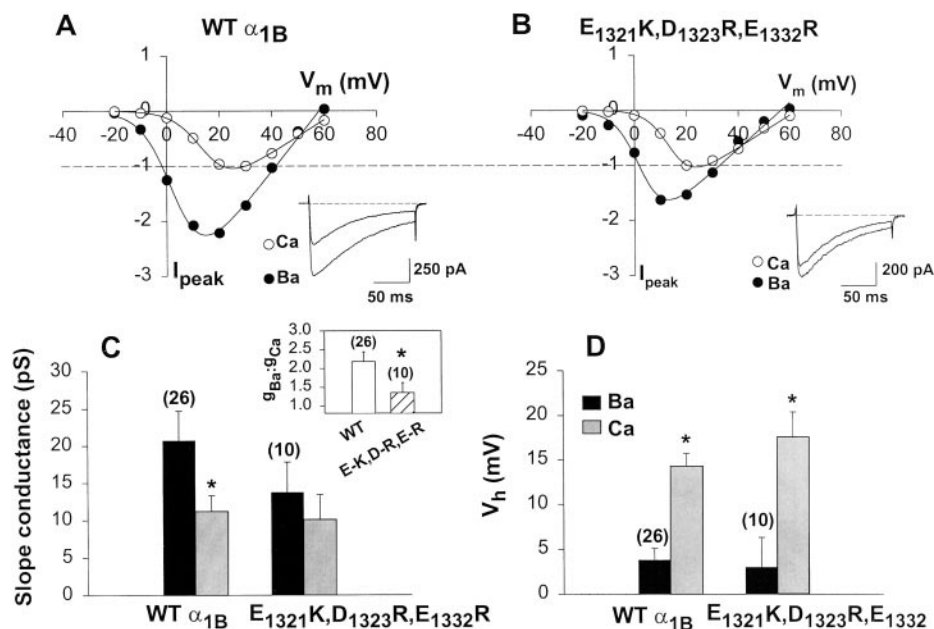


FIG. 2. *A* and *B*, macroscopic current-voltage relations and whole cell current traces obtained from wild type (WT) and mutant α_{1B} calcium channels (coexpressed with β_{1b} and $\alpha_2\delta$) with either 20 mM barium or 20 mM calcium as the external charge carrier. Note that substitution of calcium for barium reduces peak current amplitude and slope conductance of wild type channels to a greater degree compared with the α_{1B} (E1321K,D1323R,E1332R) mutant. The current records were obtained at a test potential of +30 mV. *C*, maximum slope conductance of wild type and mutant N-type calcium channels in 20 mM barium and 20 mM calcium. *Inset*, ratio of Ba:Ca conductance for the wild type and mutant calcium channels in paired experiments. Note that in the mutant channel the Ba:Ca conductance relation is significantly decreased. *D*, effect of the external charge carrier on half-activation potential obtained from fits to macroscopic current-voltage relations. In both wild type and mutant channels, replacement of barium with calcium results in a similar positive shift in half-activation potential. All error bars denote standard errors, and numbers in parentheses reflect the number of experiments.

that certain types of high voltage-activated calcium channels may contain an EF hand calcium binding motif at a region close to the outer vestibule of the pore, which is illustrated in the proposed transmembrane topography of α_1 subunit (15).

To determine whether this region of the channel could indeed be a major determinant of channel function, we used site-directed mutagenesis to replace the three conserved negative charges with a combination of arginine and lysine residues. As the template of choice, we used the N-type calcium channel α_{1B} subunit, which carries glutamic acid residues in positions 1321 and 1332 and an aspartic acid residue in position 1323. Fig. 2, *A* and *B* displays macroscopic current-voltage relations of the wild type and the α_{1B} (E1321K,D1323R,E1332R) triple mutant coexpressed in tsa-201 cells with the ancillary β_{1b} and $\alpha_2\delta$ subunits. Both the wild type and the mutant channel exhibited robust whole cell barium currents with similar half-activation and reversal potentials. Upon replacement of barium with calcium, both channels underwent a depolarizing shift in half-activation potential and an increase in peak current amplitude, but the latter effect was much more pronounced for the wild type channel compared with the triple mutant (see current records in Fig. 2). However, because of the calcium-induced shift in half-activation potential, absolute peak current values are not an ideal means of comparison. It is more accurate to compare the calcium-induced change in maximum slope conductance for the wild type and mutant channels. As shown in Fig. 2*C*, the ability of calcium ions to decrease the whole cell conductance is greatly diminished in the triple mutant, consistent with the data shown in Fig. 2, *A* and *B*. In contrast, the magnitude of the depolarizing shift in half-activation potential, which occurs when calcium is substituted for barium, was not significantly different between the wild type and the mutant channel (Fig. 2*D*). Overall, these data indicate that the domain III S5–H5 region is an important determinant of the relative whole cell barium and calcium conductances.

The whole cell conductance is a product of single channel

conductance, the total number of channels, and the maximum open probability of each channel. Thus, the data shown in Fig. 2 do not allow a clear cut mechanistic interpretation of the results. We therefore carried out cell-attached patch single channel recordings on wild type and mutant N-type calcium channels with either 100 mM barium or 100 mM calcium as the charge carrier. Similar to that previously reported in the *Xenopus* oocytes expression system (1), wild type α_{1B} (+ β_{1b} + $\alpha_2\delta$) channels display an ~60% larger single channel conductance barium conductance compared with that obtained with calcium (Fig. 3, *A* and *E*). In contrast, the single channel conductance of the triple mutant channel was similar in barium and in calcium (Fig. 3, *B* and *E*). Thus, the effects observed at the whole cell level can largely be attributed to the dependence of the single channel conductance on the nature of the charge carrier.

To determine the relative contributions of the negatively charged residues in the putative external EF hand motif, we created double (E1321K,D1323R) and a single (E1332R) mutant channels and examined their relative permeabilities for barium and calcium at the single channel level. As seen in Fig. 3, *panels C, D*, and *E*, either the double or the single substitution resulted in a reduction in the ratio of single channel barium to calcium conductance, with the single mutation having a slightly larger effect. Hence, a single amino acid substitution in the putative EF hand motif in the N-type calcium channel domain III S5–H5 region virtually abolishes the difference in barium and calcium permeability of the channel.

The data shown in Figs. 2 and 3 involve the removal of negative surface charges near the outer mouth of the pore. Hence, it is conceivable that the observed effects of these mutations on N-type calcium channel permeation could be because of a simple change in the local surface potential near the mouth of the channel. To examine this possibility, we replaced the central glycine residue (G1326) with a proline, which should introduce a major disruption into the putative EF hand motif

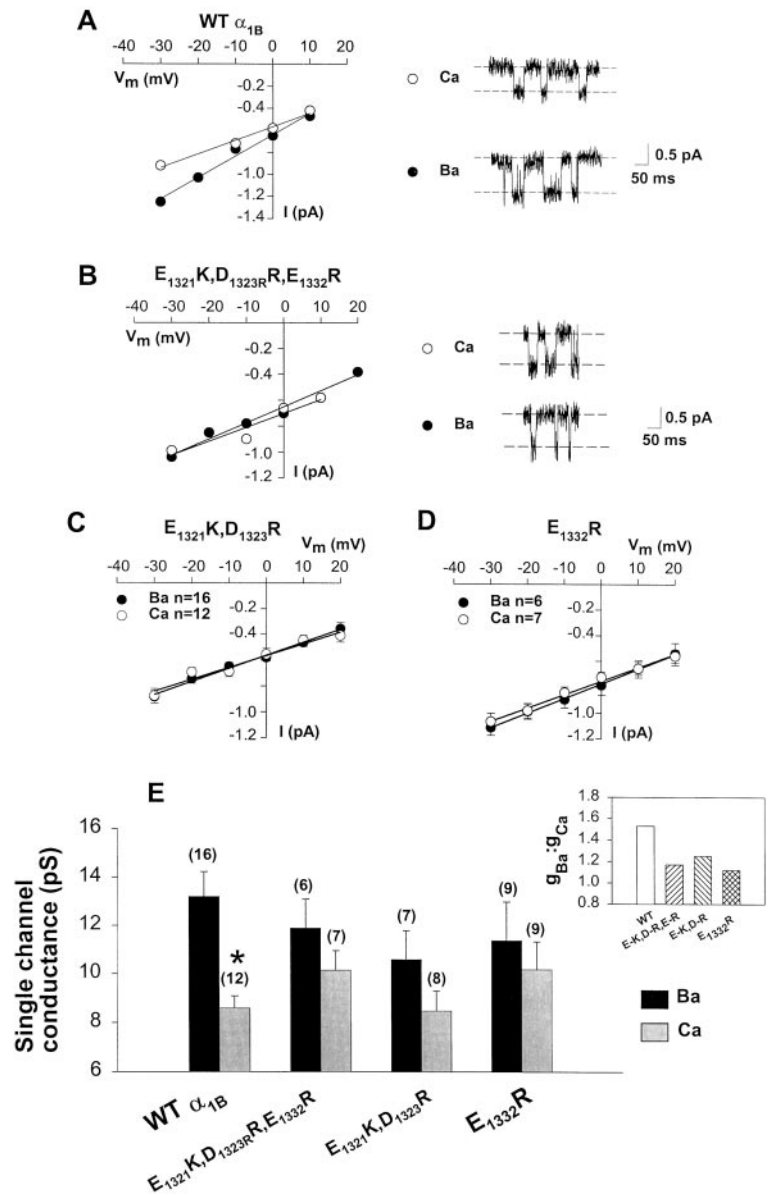


FIG. 3. *A* and *B*, single channel current-voltage relations and current records obtained with wild type (WT) and $E_{1321}K, D_{1323}R, E_{1332}R$ mutant N-type calcium channels in either 100 mM barium or 100 mM calcium. The single channel records were obtained at a test potential of 0 mV. Current-voltage relations shown are from the same experiment as the current records. Note that the mutations abolish the difference in single channel barium and calcium conductances seen with the wild type channel. *C* and *D*, effect of double $E_{1321}K, D_{1323}R$ and single $E_{1332}R$ substitutions on single channel conductance in barium and calcium. The graphs contain data from several cells, and the error bars denote standard errors. *E*, summary of the single channel barium and calcium conductances of the wild type and mutant channels. Note that only the wild type channels display significant differences in their abilities to conduct barium and calcium. Asterisks denote statistical significance, error bars indicate standard errors, and numbers in parentheses reflect number of experiments. Inset, mean Ba:Ca single conductance ratios of the wild type and mutant channels.

without changing the net charge. This mutant expressed well at the whole cell level, and showed half-activation and half-inactivation potentials that did not differ significantly from the wild type channels, indicating that the proline substitution did not affect the overall global conformation of the channel (not shown). Fig. 4A shows single channel current-voltage relations obtained from the G1326P mutant in either 100 mM barium or 100 mM calcium. As is evident from the figure, the proline substitution resulted in equal permeabilities of the N-type channel for barium and calcium ions, consistent with the hypothesis. Moreover, this effect appeared to be due to a selective increase in calcium permeability with no significant effect on barium permeation (Fig. 4B), suggesting that the intact EF hand motif may selectively decrease calcium permeability. That the difference in calcium and barium conductance can be abolished by mutagenesis of four different residues in the putative EF hand motif suggests that this region is indeed an important factor in ion permeation of the N-type calcium channel.

It has been widely accepted that the structural determinants that define the permeation characteristics of voltage-gated cation channels are localized within the four p-loop motifs of the channels (for review see Ref. 16). Crystal structure data ob-

tained from inward rectifier potassium channel clearly support a critical role of the p-loops in ion selectivity (17), although the exact side chain orientation of the selectivity filter may differ between potassium and calcium channels (11). In calcium channels, a single glutamic acid residue within each of the four p-loop motifs has been shown to be critical for divalent cation permeation (5, 6, 8, 9). It has been proposed that these glutamate residues cooperatively form two separate sites that allow a high affinity interaction between the channel and permeating ions and that electrostatic repulsion between the ions bound to those sites ultimately drives the ions across the pore (6, 8, 18). In addition, amino acid residues near the glutamate residues in domain III appear to affect ion permeation (7). Thus, the four p-loop motifs appear to be the most essential structures involved in ion permeation. Our current data do not challenge this basic principle but rather suggest the presence of other structural determinants that modulate calcium channel permeation. The putative EF hand motif in domain III region begins 10 residues 3' to the end of the S5 segment, and terminates 35 residues 5' to the critical p-loop glutamate (13), thus it seems unlikely that this region could be part of the narrow region of the channel pore.

Point mutations in the putative EF hand domain did not

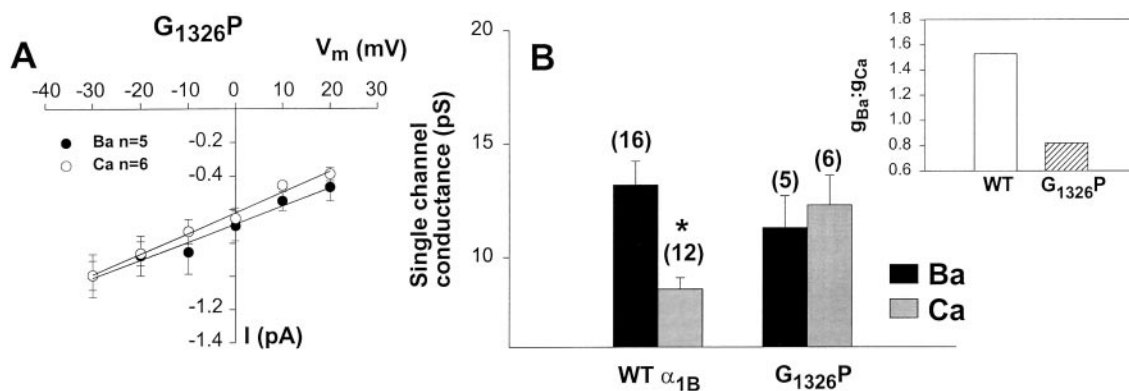


FIG. 4. *A*, effect of disruption of the putative EF hand sequence via proline substitution of the central glycine. The G1326P mutant displays similar single channel barium and calcium conductances. *B*, bar graphs illustrating the single channel conductance obtained with the wild type (*wt*) channel and the G1326P mutant (coexpressed with β_{1b} and $\alpha_2\delta$) in either 100 mM barium or 100 mM calcium. Note that the single channel conductances for barium and calcium are increased in the E1332P mutant. Error bars indicate standard errors, numbers in parentheses reflect numbers of experiments, and asterisks denote statistical significance. Inset, barium:calcium single channel conductance ratios for the wild type channel and G1326P mutant.

affect the basic biophysical properties of the channels, such as channel kinetics or the voltage dependences of activation and inactivation, and in particular the G1326P mutation did not significantly affect barium conductance of the channel. Furthermore, the IC_{50} values for cadmium block of the triple E mutant ($1.24 \pm 0.1 \mu M$, $n = 5$) and the G1326P mutant ($1.69 \pm 0.18 \mu M$, $n = 5$) did not differ significantly ($p > 0.05$) from that obtained with the wild type channel ($1.54 \pm 0.17 \mu M$, $n = 5$), indicating that the amino acid substitutions in the putative EF hand motif did not affect the narrow region of the pore. Overall, these considerations suggest that the mutations resulted in a localized structural disruption within the domain III S5–H5 region rather than mediating a global conformational change in the channel protein. We can also rule out an effect on the local electrostatic potential of the channel. Firstly, the proline mutation did not result in any change in net surface charge of the channel, and yet, calcium conductance was changed. Secondly, the net change in six charges occurring in the triple mutant increased the calcium conductance of the channel, which is opposite to that expected from a mechanism where the negative charges would serve to concentrate permanent divalent cations near the mouth of the pore. Furthermore, a diffuse surface charge effect should equally affect barium and calcium ions, but that was not observed. It is also unlikely that our observations are because of a purely allosteric effect of the point mutations on the pore region *per se*, because they selectively increased calcium conductance while leaving barium permeability relatively unaffected, and because different mutations spanning a stretch of 11 residues all had similar effects on permeation.

The calcium channel α_1 subunit has not yet been accessible to structural analysis via x-ray crystallography or NMR. In the absence of detailed structural information, it is difficult to unequivocally prove that the identified region serves as an EF hand calcium binding domain in the intact channel. Nonetheless, our data are consistent with a model in which the region could be allosterically linked to the permeation pathway of the channel. In this scenario, selective binding of calcium to the putative EF hand could result in a localized conformational change in the channel, ultimately resulting in a reduction in calcium conductance. Barium may either not bind to this region or may be incapable of changing channel conformation, thus lacking an antagonistic effect on permeation. Point mutations in this region would selectively remove the inhibitory effect of calcium ions, thus increasing calcium conductance to the levels observed with barium. Such a mechanism would support the observations that T-type calcium channels display approxi-

mately equal single channel conductances in barium and calcium, because T-type calcium channels lack the putative EF hand region (19–21). On the other hand, the putative EF hand motif is conserved in R-type (α_{1E}) calcium channels, and yet calcium and barium permeate these channels equally well (1). However, in different types of high voltage-activated calcium channels there is little sequence identity in the stretch of residues between the EF hand motif and the pore glutamate, and hence it is possible that a putative allosteric coupling between the EF hand and the pore region could be weaker or absent in α_{1E} .

Overall, our data can be explained by the involvement of a functional EF hand calcium binding region located at the extracellular side of the channel. Although detailed structural data will ultimately be required to substantiate the hypothesis, our data provide the first evidence of an involvement of non-pore residues in the permeation characteristics of voltage-dependent calcium channels.

REFERENCES

- Bourinet, E., Zamponi, G. W., Stea, A., Soong, T. W., Lewis, B. A., Jones, L. P., Yue, D. T., and Snutch, T. P. (1996) *J. Neurosci.* **16**, 4983–4993
- Hille, B. (1992) *Ionic Channels of Excitable Membranes*, 2nd Ed., Sinauer Associates, Inc., Sunderland, MA
- Hess, P., Lansman, J. B., and Tsien, R. W. (1986) *J. Gen. Physiol.* **88**, 293–319
- Carbone, E., and Lux, H. D. (1987) *J. Physiol.* **386**, 571–601
- Tang, S., Mikala, G., Bahinski, A., Yatani, A., Varadi, G., and Schwartz, A. (1993) *J. Biol. Chem.* **268**, 13026–13029
- Yang, J., Ellinor, P. T., Sather, W. A., Zhang, J. F., and Tsien, R. W. (1993) *Nature* **366**, 158–161
- Williamson, A. V., and Sather, W. A. (1999) *Biophys. J.* **77**, 2575–2589
- Ellinor, P. T., Yang, J., Sather, W. A., Zhang, J. F., and Tsien, R. W. (1995) *Neuron* **15**, 1121–1132
- Cibulsky, S. M., and Sather, W. A. (2000) *J. Gen. Physiol.* **116**, 349–362
- Heinemann, S. H., Terlau, H., Stuhmer, W., Imoto, K., and Numa, S. (1992) *Nature* **356**, 441–443
- Wu, X. S., Edwards, H. D., and Sather, W. A. (2000) *J. Biol. Chem.* **275**, 31778–31785
- Zamponi, G. W., and Snutch, T. P. (1996) *Pflugers Arch.* **431**, 470–472
- Stea, A., Soong, T. W., and Snutch, T. P. (1995) in *Handbook of Receptors and Channels: Ligand- and Voltage-gated Ion Channels* (North, R. A., ed) pp. 113–141, CRC Press, Inc., Boca Raton, FL
- da Silva, A. C., and Reinach, F. C. (1991) *Trends Biochem. Sci.* **16**, 53–57
- Catterall, W. A. (1998) *Cell Calcium* **24**, 307–323
- Sather, W. A., Yang, J., and Tsien, R. W. (1994) *Curr. Opin. Neurobiol.* **4**, 313–323
- Doyle, D. A., Morais Cabral, J., Pfuetzner, R. A., Kuo, A., Gulbis, J. M., Cohen, S. L., Chait, B. T., and MacKinnon, R. (1998) *Science* **280**, 69–77
- Hess, P., and Tsien, R. W. (1984) *Nature* **309**, 453–456
- Perez-Reyes, E., Cribbs, L. L., Daud, A., Lacerda, A. E., Barclay, J., Williamson, M. P., Fox, M., Rees, M., and Lee, J. H. (1998) *Nature* **391**, 896–900
- Cribbs, L. L., Lee, J. H., Yang, J., Satin, J., Zhang, Y., Daud, A., Barclay, J., Williamson, M. P., Fox, M., Rees, M., and Perez-Reyes, E. (1998) *Circ. Res.* **83**, 103–109
- Lee, J. H., Daud, A. N., Cribbs, L. L., Lacerda, A. E., Pereverzev, A., Klockner, U., Schneider, T., and Perez-Reyes, E. (1999) *J. Neurosci.* **19**, 1912–1921